Rare Metal Materials and Engineering
Volume 47, Issue 10, October 2018
Online English edition of the Chinese language journal

Available online at www.sciencedirect.com
ScienceDirect

Cite this article as: Rare Metal Materials and Engineering, 2018, 47(10): 2957-2963.

ARTICLE

Effect of Zn Content on the Microstructure and Mechanical Properties of the Extruded Mg-6Gd-4Y (wt%) Alloy

Zhen Rui[1,2], Sun Yangshan[3], Shen Xuewei[1]

[1] Nanjing Institute of Technology, Nanjing 211167, China; [2] Jiangsu Key Laboratory of Advanced Structural Materials and Application Technology, Nanjing 211167, China; [3] Jiangsu Key Laboratory of Advanced Metallic Materials, Southeast University, Nanjing 211189, China

Abstract: Microstructures and mechanical properties of the Mg-6Gd-4Y (wt%) alloys with and without 1wt% Zn additions were investigated. The results show that the as-cast microstructure of the Mg-6Gd-4Y alloy consist of α-Mg matrix and $Mg_{24}(GdY)_5$ secondary phase. However, the as-cast microstructure of the Zn-containing Mg-6Gd-4Y-1Zn alloy consist of α-Mg matrix, $Mg_{24}(GdY)_5$ secondary phase and $Mg_{12}Y_1Zn_1$ phase which has a 18R long period staking ordered (18R-LPSO) structure. After extrusion a 14H-LPSO phase is found in the Zn-containing alloy which is distributed between the 18R-LPSO strips in the as extruded microstructure. The formation mechanism of the 14H-LPSO phase is precipitation, and the reaction can be expressed as 'α-Mg′ → α-Mg+14H'. Zn content has no obvious effect on the precipitation of β series. Aged (T6 and T5 treatment) conducted on both the Mg-6Gd-4Y alloy and the Mg-6Gd-4Y-1Zn alloy causes the formation of β' precipitates. The T6-aged Mg-6Gd-4Y-1Zn alloy exhibits high tensile strength combined with good ductility, and the values of the yield strength (YS), ultimate tensile strength (UTS) and elongation are 309 MPa, 438 MPa and 6.8%, respectively. It is due to the coexistence of 18R-LPSO phase and finely dispersed distribution of the 14H-LPSO phase and the β' precipitates in the microstructure.

Key words: magnesium alloy; long period stacking ordered structures (LPSO); hot extrusion; aging; tensile strength

At the beginning of this century, the finding on magnesium alloys containing rare earth elements and a small amount of zinc attracted great attention of academia as well as industries since the mechanical properties of the alloys reached a higher level in comparison with commercial magnesium alloys. The excellent mechanical properties shown by the rapidly solidified powder metallurgy (RS P/M) magnesium alloys seem to originate both in grain refinement and a long period staking ordered structure (LPSO) formed in microstructure of the alloys[1].

A number of Mg-RE alloys containing a small amount of Zn have been investigated for recent ten years. These investigations have shown that the addition of a small amount of Zn can not only regulate the aging precipitation structure of Mg-RE alloy, but also form a long period ordered structure phase in Mg-RE-Zn alloy under the condition of proper addition and processing conditions [2-5]. Moreover, the additions of Zn can be used to improve mechanical properties due to the formation of long period stacking ordered (LPSO) structure which can retard the movement of the dislocations[6-9]. However, the formation conditions and the transformation mechanism of the LPSO structure phase appearing in the Mg-RE-Zn alloy system have not yet been fully understood and unified. Some researchers found that only the 18R-LPSO structure was formed in the as-cast microstructure of Mg-Y-Zn alloy system. When the alloy was heat-treated or thermally deformed at temperatures above 623 K, it was considered that the 18R-LPSO phase gradually changed to the 14H-LPSO phase[10-12]. Liu et al[13] investigated the microstructural evolution of a 18R single phase alloy during annealing at 773 K, and pointed out that the formation of 14H phase in this alloy is not transformed from 18R phase, and its formation mechanism could be explained as α-Mg′ →

Received date: October 28, 2017
Foundation item: Research Foundation of Nanjing Institute of Technology (ZKJ201604); Innovative Foundation Project for Students of Nanjing Institute of Technology (TB201702004) ; Outstanding Scientific and Technological Innovation Team in Colleges and Universities of Jiangsu Province
Corresponding author: Zhen Rui, Ph. D., Associate Professor, School of Materials Engineering, Nanjing Institute of Technology, Nanjing 211167, P. R. China, Tel: 0086-25-86118274, E-mail: 20762129@qq.com

α-Mg+14H. In addition, it has been found that 14H-LPSO structure appears in the matrix of as-cast Mg-Gd-Zn alloy system[14-17].

In the present work, the microstructures and mechanical properties of the Mg-6Gd-4Y (GW64) and Mg-6Gd-4Y-1Zn (GWZ641) alloys prepared by conventional casting and extrusion have been investigated. The 18R-LPSO and 14H-LPSO structures have been found in the Zn-containing (GWZ641) alloy, and high strength combined with relatively good ductility has been obtained from the alloy after solution treatment and aging. The formation and development of the LPSO phases in the alloy and their strengthening mechanism have been also studied.

1 Experiment

The alloy ingots with nominal composition of Mg-6Gd- 4Y (wt%) and Mg-6Gd-4Y-1Zn (wt%) were prepared using pure Mg, Gd, Y and Zn stocks. Melting of the alloy was conducted in a mild steel crucible under the protective gas of CO_2 and SF_6 with the ratio of 100:1. After the alloying elements were dissolved, the melt was held at 993 K for 10 min, and then poured into a water cooled mold made of cast copper. The cylindrical ingots with a diameter of 60 mm, were annealed for homogenization at 783 K for 12 h, and then hot extruded at 603 K with extrusion ratio of 9:1. Some of the extruded rods were solution treated (T4) at 793 K for 6 h and quenched into cold water. Aging was conducted on both as- extruded and solution treated specimens at 498 K.

Microstructural characterization was conducted in the cross section of the processed zone by X-ray diffraction (XRD), scanning electron microscopy (SEM) and transmission electron microscopy (TEM). Tensile tests were carried out using the CMT-5105 tensile testing machine at a speed of 2 mm/min at room temperature.

2 Results and Discussion

2.1 Microstructure

Fig.1 shows XRD patterns of the as-cast specimens of GW64 and GWZ641 alloys. The as-cast GW64 alloy consist mainly of α-Mg solid solution together with $Mg_{24}(GdY)_5$ secondary phase. However, the XRD results of the as-cast alloy GWZ641 show that phase constituents includes α-Mg solid solution, $Mg_{24}(GdY)_5$ and $Mg_{12}Y_1Zn_1$ secondary phases.

The microstructures of the as-cast specimens of GW64 and GWZ641 alloys are shown in Fig.2a and 2b, respectively. It can be seen that the as-cast GW64 alloy microstructure consists of α dendrites and an interphase networks, which can be identified as $Mg_{24}(GdY)_5$ according to the XRD pattern shown in Fig.1a. But in GWZ641 alloy, some lamellae phase is observed, which can be identified as $Mg_{12}Y_1Zn_1$ according to the XRD pattern shown in Fig.1b.

Fig.3a and 3b show the TEM image of the $Mg_{12}Y_1Zn_1$ phase in as cast specimens of the GWZ641 alloy and the corresponding selected area electron diffraction (SAED) pattern, respectively. The SAED pattern demonstrates that the $Mg_{12}Y_1Zn_1$ phase has a 18R-type structure. It shows that Zn content is a necessary condition for the formation of 18R-LPSO in the alloy studied.

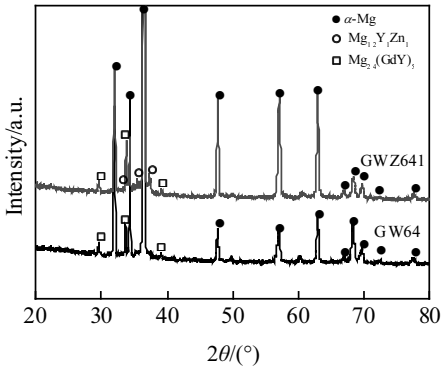

Fig.1 XRD patterns of the as-cast alloys

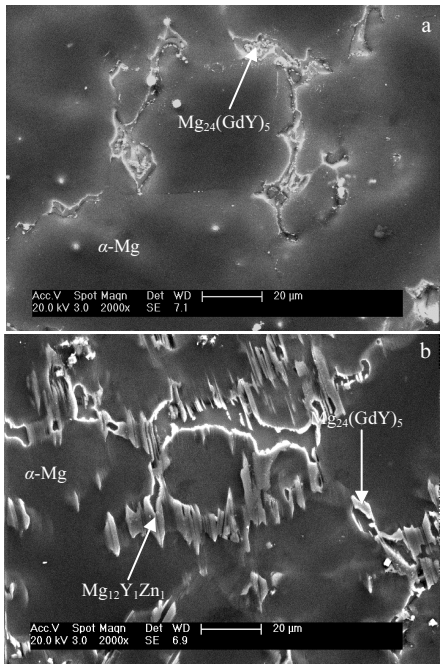

Fig.2 SEM images of the as-cast alloys: (a) GW64 and (b) GWZ641

Fig.4a and 4b show SEM micrographs of the as-extruded alloys GW64 and GWZ641, respectively. It can be seen that the $Mg_{24}(GdY)_5$ eutectic networks in the as-cast GW64 alloy are destroyed and the broken particles are distributed along the extrusion direction, and the $Mg_{12}Y_1Zn_1$ phases which has a 18R-LPSO structure in the as-cast GWZ641 alloy is stretched along the direction of extrusion. It is evident that the matrix grains in the as-extruded are very fine in comparison with that in the as-cast microstructure (Fig.2), indicating recrystallization

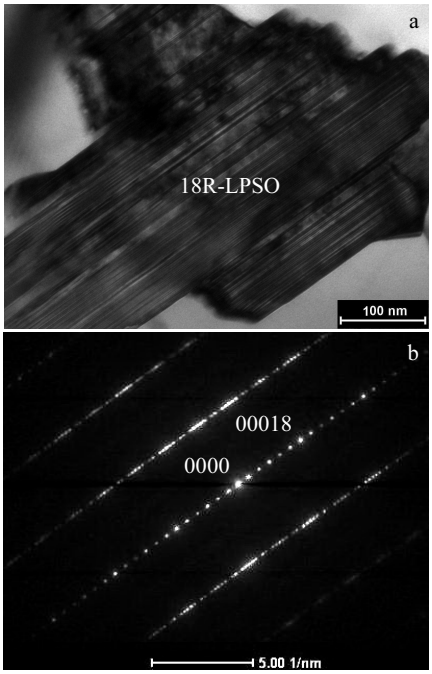

Fig.3 TEM image of the $Mg_{12}Y_1Zn_1$ phase (a) and corresponding SAED (EB//$[11\bar{2}0]_\alpha$) pattern (b) in the as-cast GWZ641 alloy

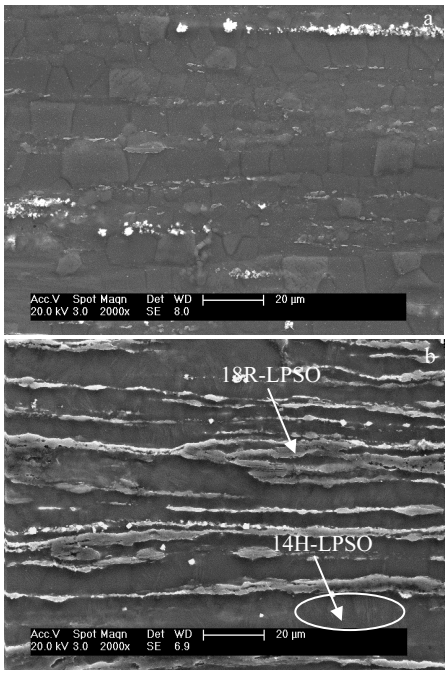

Fig.4 SEM images of the as-extruded alloys: (a) GW64 and (b) GWZ641

occurred during extrusion. However, there are no cracks large enough to be observed within the kinked 18R-LPSO lamellas or at the interface between 18R-LPSO phase and α-Mg matrix (shown in Fig.4b), demonstrating excellent ductility of 18R-LPSO phase. In addition, much more fine lamellae can be observed in as-extruded GWZ641 alloy microstructure, as shown in Fig.4b.

The morphology details of the fine lamellae are revealed by TEM observations. Fig.5a is the TEM bright field image taken from the area of fine lamellae in the as-extruded specimen of the GWZ641 alloy, and the corresponding SAED pattern taken along $[11\bar{2}0]$ zone axis is shown in Fig.5b. Both of them are identified as arising from the typical 14H-LPSO structure.

Grobner et al. investigated the occurrence and transformations of long-period stacking ordered structures 18R and 14H in as-cast and heat-treated Mg-Y-Zn alloys and reported[10] that the 18R structure is a stable equilibrium phase that forms directly from the melt whereas the 14H cannot form directly from the melt but forms in a solid-state transformation. Grobner et al. found that the 18R is a stable equilibrium phase that exists in the high temperature range from 1026 K to 756 K, and that the 14H is an equilibrium phase below 810 K. The 18R-LPSO phase is observed not only in the rapidly solidified samples, but also in samples produced by the conventional casting methods such as permanent mold casting[12,18-21]. Combined with the 18R-LPSO phase formed in the as-cast microstructure of Mg-6Gd-4Y-1Zn alloy studied in the present work, it can be concluded that the 18R-LPSO phase can be formed directly from the liquid metal in a very wide range of cooling rates.

However, there is no unified view on the formation of 14H-LPSO phase of the ternary Mg-Y-Zn and quaternary

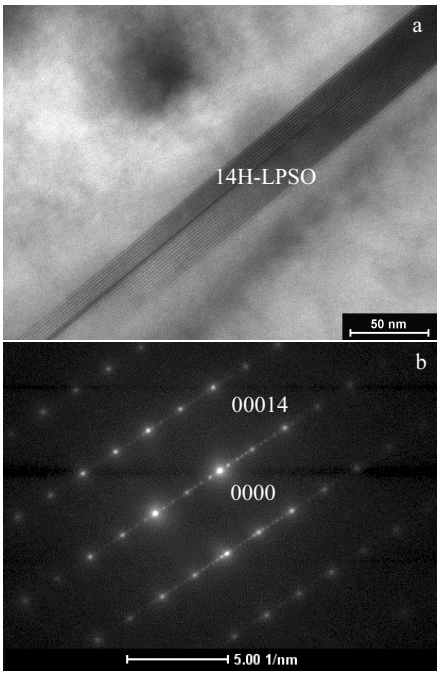

Fig.5 TEM image (a) and corresponding SAED (B//$[11\bar{2}0]_\alpha$) pattern (b) of the as-extruded GWZ641 alloy

Mg-Gd-Y-Zn alloys after annealing at high temperature. It is believed that the 14H-LPSO phase is converted from the 18R-LPSO phase formed in the as-cast state[3,9,12,18,22]. These views can partly explain why the new formation of Mg-Y-Zn alloy in the 14H layer and 18R have a specific orientation relationship, but cannot reasonably point out the type of 18R→14H solid phase transitions and reaction equations. In the present work, there are two types of LPSO structures of 14H and 18R in the microstructure of the extruded Mg-6Gd-4Y-1Zn alloy (Fig.4b). And the volume fraction of the $Mg_{12}Y_1Zn_1$ phase with 18R-LPSO structure is not reduced compared with the as-cast microstructure (Fig.2b). In addition, the 14H-LPSO phase in the Mg-6Gd-4Y-1Zn alloy is not only formed around the 18R-LPSO phase, but randomly distributed in the different positions of the α-Mg grains to nucleate and grow gradually (Fig. 4b and Fig. 6b). Therefore, the experimental results of the present work do not support the view that the 18R phase is directly transformed into 14H phase. It is considered that there is little possibility for the direct conversion of 18R-LPSO to 14H-LPSO in the system. The results of microstructure observation in the present work support the precipitation mechanism for the formation of 14H-LPSO in the Mg-Gd-Y-Zn alloy, and the reaction can be expressed as 'α-Mg′ → α-Mg + 14H'.

Fig.6a and 6b show the SEM images of peak-aged specimens of the extruded-T6 alloys studied. In comparison with the as extruded microstructure shown in Fig.4, it is found that solid solution treatment of extruded GW64 and GWZ641 alloys at high temperature above 793 K results in the dissolution of intermetallics into the matrix (Fig.6a and 6b) and the precipitation of the 14H-LPSO phase through the α-matrix grains (shown in Fig.6b). Meanwhile, 14H-LPSO phase can be observed in the extruded-T6 GWZ641 alloy, indicating the 14H-LPSO phase formed during solution treatment is stable and remains in the microstructure of the alloy after aging. Fig.6c and 6d are the TEM micrographs taken from the GW64 and GWZ641 alloys after T6 aging treatment, from which β' precipitates can be observed.

Aging has also been conducted on as extruded specimens (T5 treatment) of the alloy without solid solution treatment. Fig. 7a and 7b show the SEM micrographs taken from T5 treated specimens of the GW64 and GWZ641 alloys, respectively. In comparison with Fig. 6, it is found that the volume fraction of the 14H-LPSO phase in the GWZ641 alloy is much lower in the T5 treated specimen than that in the T6 aged specimens, as shown in Fig.6b and Fig.7b~7d show the TEM images taken from T5 aged specimens of the GW64 and GWZ641 alloys. It can be seen that aging conducted (T6 and T5 treatment) on both the Mg-6Gd-4Y alloy and the Mg-6Gd-4Y-1Zn alloy caused the formation of β' precipitates. Thus, Zn content has no obvious effect on the precipitation of β series. Both 14H-LPSO phases and β' precipitates exist in the microstructure of the T5 treated GWZ641 alloys (shown in Fig.7d), but the volume fraction of the β' precipitates is lower than that in the T6 treated specimens (shown in Fig.6d).

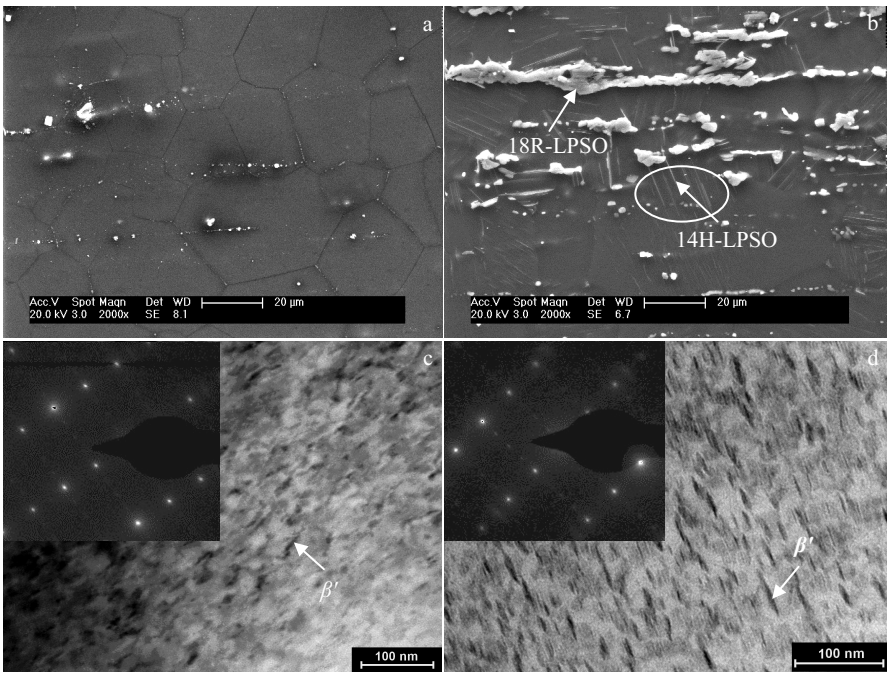

Fig.6 Microstructures of the peak-aged extruded-T6 alloy: (a) SEM image of GW64, (b) SEM image of GWZ641, (c) TEM image and SAED pattern of β' phase in GW64, and (d) TEM image and SAED pattern of β' phase in GWZ641

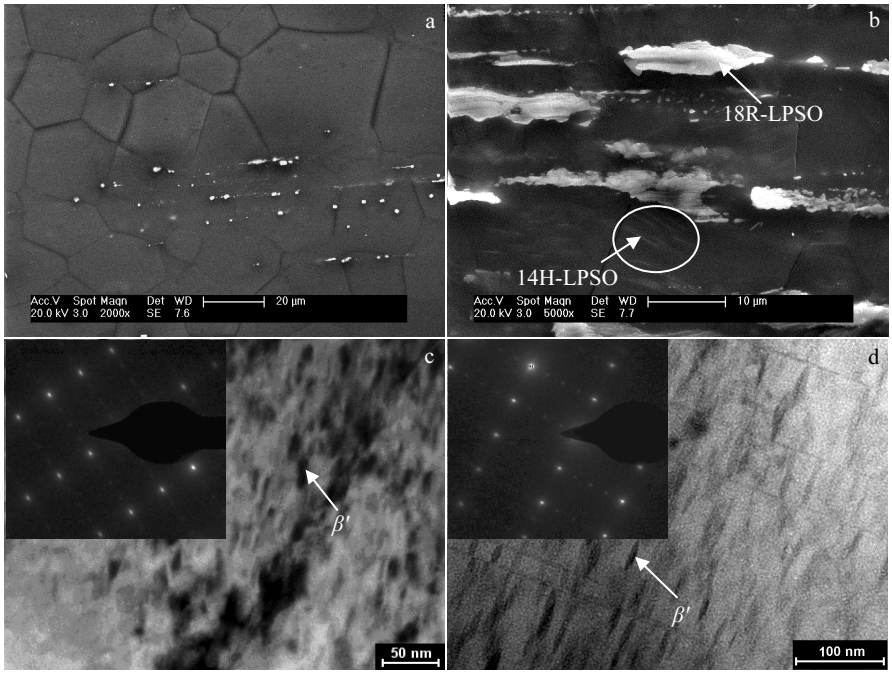

Fig.7 Microstructures of the peak-aged extruded-T5 alloy: (a) SEM image of GW64, (b) SEM image of GWZ641, (c) TEM image and SAED pattern of β' phase in GW64, and (d) TEM image and SAED pattern of β' phase in GWZ641

2.2 Tensile properties

A comparison of the typical mechanical properties of the two alloys in different states is listed in Table 1. Tensile tests at room temperature reveal that the strengths and elongation of as-cast Mg-6Gd-4Y and Mg-6Gd-4Y-1Zn alloys are relatively low. However, both the strengths and ductility of the two alloys are remarkably improved after extrusion, especially for the GWZ641 alloy, as shown in Table 1. The values of UTS and YTS of the GWZ641 alloy in the as- extruded condition are about 342 and 232 MPa, respectively, with a good elongation of 7.4%. Compared with the GWZ641 alloy in as-cast condition, the UTS is improved by 206 MPa, and the increment of YTS is 112 MPa. The increase in mechanical properties after extrusion is mainly attributed to micro-structure refining, which is the result of recrystallization occurring during hot extrusion. Further improvement on tensile properties is achieved by aging. Both T5 and T6 treatments result in significant increase of both ultimate and yield strength and the highest ultimate strength of the two alloys. High yield strength (309 MPa), high tensile strength (438 MPa) combined with good ductility (6.8%) is obtained from the GWZ641 alloy after T6 aging.

Table 1 Tensile properties of the Mg-6Gd-4Y and Mg-6Gd-4Y- 1Zn alloy at room temperature

Alloys state	GW64			GWZ641		
	σ_b/MPa	$\sigma_{0.2}$/MPa	δ/%	σ_b/MPa	$\sigma_{0.2}$/MPa	δ/%
As-cast	124	102	2.5	136	120	2.2
Extruded	265	181	4.7	342	232	7.4
T6	303	212	4.0	438	309	6.8
T5	350	256	1.2	397	260	4.6

Note: T6, T5— peak-aged

From this investigation, it can be seen that the tensile strength and elongation of the extruded, T5 treated and T6 treated Mg-6Gd-4Y-1Zn alloy are higher than those of Mg-6Gd-4Y alloy without Zn content. After T6 treatment, in particular the tensile strength of GWZ641 alloy is 44.6% higher than that of GW64 alloy. It can be concluded that the LPSO phase plays an important role in strengthening mechanisms for Mg-Gd-Y-Zn alloys. Fig.8 is the TEM image of the Mg-6Gd-4Y-1Zn specimen after tensile test. It can be seen that there are many dislocations stacked around the 18R-LPSO and 14H-LPSO phase, indicating that the LPSO phase can strengthen the alloy by preventing the dislocation movement.

In addition, most previous investigations show that the improvement effect of T5 treatment on the mechanical properties of Mg-RE(-Zn) alloy is better than that of T6 treatment. In the present investigation, strength of T5 treated Mg-6Gd-4Y specimen is higher than that of the T6 treated. This is probably because of the unavoidable microstructure coarsening occurring during solution treatment, which is prior to aging for T6 treatment. However, the strengths and ductility of the Mg-6Gd-4Y-1Zn alloy after T6-aging are higher than that of the alloy after T5 aging, as shown in Table 1. It can be seen that the volume fraction of both 14H-LPSO phase and β' precipitates in the T6 treated specimen (Fig.6b and 6d) are

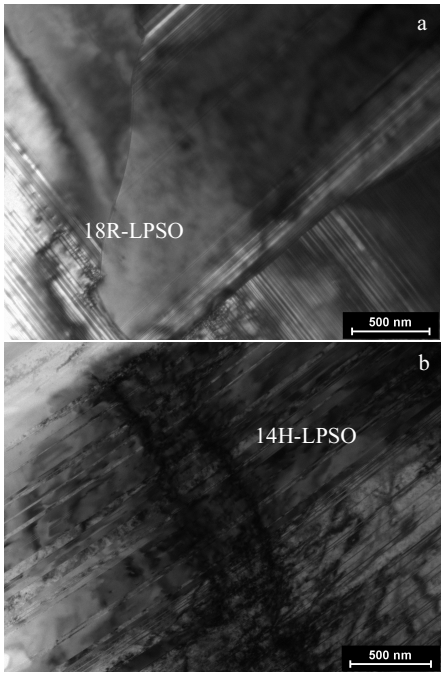

Fig.8 TEM micrographs of 18R-LPSO (a) and 14H-LPSO (b) structure in as-extruded GWZ641 alloy after tensile test

higher than that in the T5 treated specimens (Fig.7b and 7d). It was reported (by M. Yamasaki et al.[7]) that formation of the 14H-LPSO occurred at a temperatures above 623 K, which is much higher than aging temperature of T5 treatment (498 K) in the present investigation. For T5 treatment, aging was conducted on as-extruded alloy without prior solution treatment;, hence, the volume fraction of 14H-LPSO was lower than that in the T6 treated specimen. It is suggested that the 14H- LPSO phase not only enhances the tensile strength, but also improves the deformation plasticity. In addition, as seen for Table 1, the elongation for T5-treated GW64 alloy is lower than that at the as-cast stage. However, the elongation for T5-treated GWZ641 alloy which has the 14H-LPSO phase is much higher than that at the as-cast stage. From this investigation, it can be concluded that the coexistence of 18R-LPSO phase and finely dispersed distribution of the 14H-LPSO phase and the β' precipitates in the microstructure achieves the ideal strengthening effect.

3 Conclusions

1) The as-cast microstructure of the Mg-6Gd-4Y alloy studied consists of the α-Mg matrix and $Mg_{24}(GdY)_5$ secondary phase. However, the as-cast microstructure of the Zn-containing Mg-6Gd-4Y-1Zn alloy consists of α-Mg matrix, $Mg_{24}(GdY)_5$ secondary phase and $Mg_{12}Y_1Zn_1$ phase which has a 18R long period staking ordered (18R-LPSO) structure.

2) After extrusion the 14H-LPSO phase is found in the Zn-containing alloy and distributed between the 18R-LPSO strips in the as extruded microstructure. The formation mechanism of the 14H-LPSO phase is precipitation, and the reaction can be expressed as 'α-Mg′ → α-Mg + 14H'.

3) Zn content has no obvious effect on the precipitation of β series. Aging conducted (T6 and T5 treatment) on both the Mg-6Gd-4Y alloy and the Mg-6Gd-4Y-1Zn alloy causes the formation of β' precipitates.

4) The T6-aged Mg-6Gd-4Y-1Zn alloy exhibits high tensile strength combined with good ductility, and the values of the yield strength (YS), ultimate tensile strength (UTS) and elongation are 309 MPa, 438 MPa and 6.8%, respectively. It is due to the coexistence of 18R-LPSO phase and finely dispersed distribution of the 14H-LPSO phase and the β' precipitates in the microstructure.

References

1 Kawamura Y, Hayashi K, Inoue A *et al. Materials Transactions*[J], 2001, 42(7): 1172
2 Wu Y J, Zeng X Q, Lin D L *et al. Journal of Alloys and Compounds*[J], 2009,477(1-2) : 193
3 Liu K, Rokhlin L L, Elkin F M *et al. Materials Science and Engineering A*[J], 2010, 527(3): 828
4 Liu Huan, Xue Feng, Bai Jing *et al. Rare Metal Materials and Engineering*[J], 2014, 43(3): 0570
5 Li M, Zhang K, Li X G *et al*. *Materials Science and Engineering A*[J], 2015, 638(10): 46
6 Xuan Liu, Zhiqiang Zhang, Wenyi Hu *et al. Journal of Materials Science & Technology*[J], 2016, 32(4): 313
7 Yamasaki M, Sasaki M, Nishijima M *et al. Acta Materialia*[J], 2007, 55(20): 6798
8 Liu K, Zhang J, Su G *et al. Journal of Alloys and Compounds*[J], 2009, 481(1-2): 811
9 Wen Kai, Liu Ke, Wang Zhaohui *et al. Materials Science and Engineering A*[J], 2016, 674: 33
10 Gröbner J, Kozlov A, Fang X Y *et al. Acta Materialia*[J], 2012, 60(17): 5948
11 Tong L B, Li X H, Zhang H J. *Materials Science and Engineering A*[J], 2013, 563: 177
12 Zhu Y M, Morton A J, Nie J F. *Acta Materialia* [J], 2010, 58(8): 2936
13 Liu Huan, Yan Kai, Yan Jingli *et al. Transactions of Nonferrous Metals Society of China*[J], 2017, 27(1): 63
14 Wu Y J, Lin D L, Zeng X Q *et al*. *Journal of Materials Science* [J], 2009, 44(6): 1607
15 Zeng Xiaoqin, Wu Yujuan, Peng Liming *et al. Acta Metallurgica Sinica*[J], 2010, 46(9): 1041
16 Meng Jiao, Xue Feng, Sun Jingjing *et al. Rare Metal Materials and Engineering*[J], 2015, 44(10): 2429 (in Chinese)
17 Zhen Rui, Sun Yangshan, Xue Feng *et al. Journal of Alloys and Compounds*[J], 2013, 550(2): 273
18 Itoi T, Seimiya T, Kawamura Y *et al. Scripta Materialia*[J], 2004, 51(2): 107
19 Matsuda M, Ii S, Kawamura Y *et al. Materials Science and*

Engineering A[J], 2004, 386(1-2): 447
20 Matsuda M, Ii S, Kawamura Y *et al. Materials Science and Engineering A*[J], 2005, 393(1-2): 269
21 Zhu Y M, Morton A J, Nie J F. *Acta Materialia*[J], 2012, 60(19): 6562
22 Liu Huan, Bai Jing, Yan Kai *et al*. *Materials & Design*[J], 2016, 93: 9

Zn 含量对 Mg-6Gd-4Y 变形镁合金显微组织与力学性能的影响

甄　睿[1,2]，孙扬善[3]，沈学为[1]

(1. 南京工程学院，江苏 南京 211167)

(2. 江苏省先进结构材料与应用技术重点实验室，江苏 南京 211167)

(3. 东南大学 江苏省先进金属材料高技术研究重点实验室，江苏 南京 211189)

摘　要：研究了 Mg-6Gd-4Y (质量分数，%)合金与添加质量分数 1%Zn 的 Mg-6Gd-4Y-1Zn 合金的显微组织与力学性能。结果表明：Mg-6Gd-4Y 合金的铸态组织由α-Mg 基体和 $Mg_{24}(GdY)_5$ 两相组成。而含有 Zn 的 Mg-6Gd-4Y-1Zn 合金的铸态组织则主要由 α-Mg，$Mg_{24}(GdY)_5$ 和具有 18R-LPSO 结构的 $Mg_{12}Y_1Zn_1$ 相组成。挤压后，在含锌合金中发现了 14H-LPSO 相，分布于条状分布的 $Mg_{12}Y_1Zn_1$ 之间。14H-LPSO 相的形成机理为沉淀析出，反应可表示为 α-Mg′→α-Mg+14H。Zn 含量对 β 系列沉淀物没有明显的影响。在 Mg-6Gd-4Y 合金和 Mg-6Gd-4Y-1Zn 合金上进行的时效（T6 和 T5）处理均引起 β′析出相的形成。T6 处理后的 Mg-6Gd-4Y-1Zn 合金具有高抗拉伸强度和良好的延展性，屈服强度（YS），抗拉强度（UTS）和延伸率分别为 309 MPa，438 MPa 和 6.8%。这是 18R-LPSO 相与细小弥散分布的 14H-LPSO 相和 β′沉淀相共同作用的结果。

关键词：镁合金；长周期结构（LPSO）；热挤压；时效处理；拉伸强度

作者简介：甄　睿，女，1978 年生，博士，副教授，南京工程学院材料工程学院，江苏 南京 211167，电话：025-86118274，E-mail: 20762129@qq.com